THE JOURNAL OF BIOLOGICAL CHEMISTRY
Vol. 278, No. 40, Issue of October 3, pp. 38803–38812, 2003

Printed in U.S.A.

dUTPase and Nucleocapsid Polypeptides of the Mason-Pfizer Monkey Virus Form a Fusion Protein in the Virion with Homotrimeric Organization and Low Catalytic Efficiency*

Received for publication, June 30, 2003, and in revised form, July 15, 2003
Published, JBC Papers in Press, July 16, 2003, DOI 10.1074/jbc.M306967200

Orsolya Barabás‡§, Michaela Rumlová¶‖, Anna Erdei, Veronika Pongrácz‡, Iva Pichová¶, and Beáta G. Vértessy‡ ‡‡**

*From the ‡Institute of Enzymology, Biological Research Center, Hungarian Academy of Sciences, POB 7, H-1518, Budapest, Hungary, the §Department of Theoretical Chemistry, Eötvös Loránd University, POB 32, H-1518 Budapest, Hungary, the ¶Institute of Organic Chemistry and Biochemistry, Academy of Sciences of the Czech Republic, Prague, Czech Republic, the **Department of Immunology, Eötvös Loránd University, Budapest, Hungary, and the ‖Department of Biochemistry and Microbiology, Institute of Chemical Technology, Prague, Czech Republic*

Betaretroviruses encode dUTPase, an essential factor in DNA metabolism and repair, in the *pro* open reading frame located between *gag* and *pol*. Ribosomal frameshifts during expression of retroviral proteins provide a unique possibility for covalent joining of nucleocapsid (NC) and dUTPase within Gag-Pro polyproteins. By developing an antibody against the prototype betaretrovirus Mason-Pfizer monkey virus dUTPase, we demonstrate that i) the NC-dUTPase fusion protein exists both within the virions and infected cells providing the only form of dUTPase, and ii) the retroviral protease does not cleave NC-dUTPase either in the virion or *in vitro*. We show that recombinant betaretroviral NC-dUTPase and dUTPase are both inefficient catalysts compared with all other dUTPases. Dynamic light scattering and gel filtration confirm that the homotrimeric organization, common among dUTPases, is retained in the NC-dUTPase fusion protein. The betaretroviral dUTPase has been crystallized and single crystals contain homotrimers. Oligonucleotide and Zn^{2+} binding is well retained in the fusion protein, which is the first example of acquisition of a functional nucleic acid binding module by the DNA repair factor dUTPase. Binding of the hexanucleotide ACTGCC or the octanucleotide $(TG)_4$ to NC-dUTPase modulates enzymatic function, indicating that the low catalytic activity may be compensated by adequate localization.

The ubiquitous enzyme dUTP pyrophosphatase (dUTPase)[1] is unique in its capacity to prevent incorporation of uracil into DNA (1). dUTPase produces the dTTP precursor dUMP and decreases cellular dUTP levels, its lack leads to an elevated dUTP/dTTP ratio and DNA with a high content of uracil. Excision repair of uracil-DNA results in a futile cycle because of the low cellular dTTP content. Subsequently, multiple double-stranded DNA breaks and thymine-less cell death occur (2). dUTPase is essential in both pro- and eukaryotes (3, 4) and restricts host range and pathogenicity in both retroviruses (5–7) and *Herpesvirus* (8). Null mutations in retroviral dUTPase gene affect viral growth only in non-dividing cells (*e.g.* macrophages) (6, 9). Consequently, viral dUTPases are subjects of medical interest.

Retroviral dUTPase genes are located in non-primate lentiviruses and betaretroviruses at different genomic locations (10–12). Lentiviral dUTPase genes are in the *pol* open reading frame between reverse transcriptase and integrase genes, although in betaretroviruses, the 5′-portion of the *pro* frame encodes dUTPase. Virion lysates show dUTPase activity, indicating enzyme encapsulation in the virion (13). In betaretroviruses mouse mammary tumor virus (MMTV) (14) and Mason-Pfizer monkey virus (M-PMV) (15), two ribosomal frameshifts between *gag* and *pro* and *pro* and *pol* frames occur, yielding Gag-Pro and Gag-Pro-Pol polyproteins. The first frameshift may give rise to a transframe fusion protein joining the nucleocapsid (NC) and dUTPase polypeptides. Such a fusion protein is present in MMTV (16). The catalytic efficiency of recombinant MMTV NC-dUTPase was, however, low compared with lentiviral or other dUTPases (16, 17). The low activity was attributed to the harmful replacement of a strongly conserved tyrosine by phenylalanine in a dUTPase sequence motif (12). In this motif, Tyr is important for enzyme function (18, 19). This natural Tyr to Phe substitution prevented an independent assessment of the role of the NC domain on dUTPase activity in the MMTV transframe protein.

Eukaryotic, bacterial, and retroviral (EuBaR) dUTPases are homotrimers with three active sites, each of which is constructed by conserved sequence motifs from all the three subunits (20–23). This architecture, unique among enzymes and conserved in EuBaR dUTPases despite a low sequence similarity, provides a strong dependence of catalytic activity upon oligomerization. The nucleocapsid domain of NC-dUTPase adding 81 amino acids to the 153-residue monomer of dUTPase represents a significant N-terminal extension in the fusion protein. This might interfere with the organization of the N-terminal β-strand of M-PMV dUTPase. In human, *Escherichia coli* and lentiviral enzyme crystal structures, this segment contributes to cohesive intersubunit forces by making

* This work was supported by the Hungarian National Research Foundation (Grants T034120, TS044730, and M27852 (to B. G. V.) and T034944), the Howard Hughes Medical Institutes Grant 55000342 (to B. G. V.), the Alexander von Humboldt Foundation, the Aventis/Institut de France Scientia Europeae Prize (to B. G. V.), by Grant IAA405304 from the Grant Agency of the Academy of Sciences of the Czech Republic and Research project Z4055905 (to I. P.), and by Grant 223300006 supported by Czech Ministry of Education (to M. R.). The costs of publication of this article were defrayed in part by the payment of page charges. This article must therefore be hereby marked "*advertisement*" in accordance with 18 U.S.C. Section 1734 solely to indicate this fact.

‡‡ To whom correspondence should be addressed: Institute of Enzymology, Biological Research Center, Hungarian Academy of Sciences, POB 7, H-1518, Budapest, Hungary. E-mail: vertessy@enzim.hu.

[1] The abbreviations used are: dUTPase, dUTP pyrophosphatase; MMTV, mouse mammary tumor virus; M-PMV, Mason-Pfizer monkey virus; NC, nucleocapsid; DTT, dithiothreitol; CD, circular dichroism.

H-bonded contact with the C-terminal β-strand of the neighboring subunit (20–23). It is therefore of importance to investigate the oligomerization properties of the transframe protein in relation to the enzymatic activity.

Retroviral dUTPases may combine enzymatic function with localization and architectural roles by recruiting additional domains for interaction with nucleic acids. We have, therefore, set out to investigate the presence of NC-dUTPase in the mature M-PMV virion, together with its structural and functional characterization. We selected M-PMV instead of MMTV to circumvent the problem of Tyr to Phe replacement present in MMTV, but not in M-PMV (15). We have identified NC and NC-dUTPase in Western blots of M-PMV virions and determined their relative amounts. To assess the relative influence of the NC domain on dUTPase activity, we generated expression systems for the fusion protein as well as for dUTPase separate from the NC segment. NC-dUTPase and dUTPase were purified to homogeneity, and characterized with respect to protein structure and kinetic properties. The role of the NC segment and oligonucleotide binding in modulating dUTPase activity was investigated. Single crystals of M-PMV dUTPase suitable for x-ray diffraction analysis were generated. NC-dUTPase is shown to possess intact homotrimeric organization, ability to interact with oligonucleotides and an inherent low dUTPase activity that might be modulated upon oligonucleotide binding to the NC segment.

EXPERIMENTAL PROCEDURES

Electrophoretic materials and Chelex were from Bio-Rad, chromatographic materials from Amersham Biosciences, Phenol Red indicator from Merck, and other materials of analytical grade from Sigma. Molecular biology materials were from Stratagene, unless stated otherwise.

Plasmids, Vectors, and Bacterial Strains—The plasmid FPpSARM4, containing the whole M-PMV genome with one nucleotide insertion within frameshifting sequence between *gag* and *pro* genes, was used as a template for PCR amplification of M-PMV dUTPase and NC-dUTPase genes. The plasmid pET22b (Novagen) in the *E. coli* strain BL21(DE3)pLysS was used for protein expression. *E. coli* strains DH5α and XL1-Blue were used for plasmid amplification. Primer synthesis and DNA sequencing were performed by Generi Biotech, Hradec Králové Czech Republic, and Biological Research Center in Szeged, Hungary.

DNA manipulations were carried out by common techniques (24). Constructs were verified by DNA sequencing. M-PMV dUTPase gene was amplified by PCR using the FPpSARM4 template and the primers 5′-dUTP, 5′-CCACCCCA**CATATG**AAACGGGTGGAG-3′ (*Nde*I site fused into the start ATG codon in bold) and 3′-dUTP, TAGG**CTCGAG**TTAATATATGTCTGA (*Xho*I site and stop codon in bold). Double-digested PCR fragment was purified (QIAquick PCR purification kit) and ligated into pET22b. The resulting recombinant plasmid was named dUTPase/pET22b. For better codon usage in bacterial expression systems, two silent mutations were introduced to replace CGG^{Arg} with $CG\mathbf{T}^{Arg}$ as well as GGG^{Gly} with $GG\mathbf{T}^{Gly}$ using the primers 5′-RGdUTP: GAGATATACATATGAAACGTGTGGAGGGTCCAGC, and 3′-dUTP, and dUTPase/pET22b as a template to give plasmid RGdUTPase/pET22b. M-PMV NC-dUTPase gene was amplified using FPpSARM4 as template and the primers 5′-NCdUTP AAGGCCTGCATATGGCCGCCGCCT and 3′-dUTP to result in the plasmid NC-dUTPase/pET22b.

Expression and Purification of Recombinant NC-dUTPase and dUTPase—E. coli BL21(DE3)pLysS (25) cells transformed with the plasmids were propagated till exponential growth, then induced by 0.5 mM iso-propyl-β-D-thiogalactoside. Cells were harvested three to four hours post-induction and stored at −70 °C. Subsequent manipulations were carried out on ice. For purification of M-PMV dUTPase, cell pellets were solubilized in 1/10 volume of lysis buffer (50 mM Tris-HCl (pH 8.5) containing 150 mM NaCl, 1 mM EDTA, 1 mM dithiothreitol (DTT), and 0.5 mM phenylmethanesulfonyl fluoride and 2 μg/ml RNase and DNase). Cell suspensions were stirred for 30 min, sonicated (3–5 × 60 s), and centrifuged (18,000 × *g* for 20 min). Supernatant was dialyzed overnight against 50 mM Tris buffer (pH 6.8) containing 50 mM NaCl, 1 mM DTT, and 1 mM phenylmethylsulfonyl fluoride and loaded on a CM-Sepharose or SP-Sepharose ion exchange column (200 ml) equilibrated in the same buffer, and developed in a linear gradient of 1 M NaCl. dUTPase eluted at 0.5–0.6 M NaCl, as followed by enzyme activity measurements and SDS-PAGE. Concentrated enzyme fractions were gel filtrated on Superdex 200 HR column using 50 mM Tris buffer (pH 7.5) also containing 300 mM NaCl, 1 mM DTT, and 10 mM $MgCl_2$. Cell pellets for purification of M-PMV NC-dUTPase were solubilized as above, but in lysis buffer containing 5 mM DTT. Supernatants were directly loaded on a HiTrap Heparin HP column (5 ml), equilibrated in 50 mM Tris buffer (pH 8.0) containing 150 mM NaCl, 5 mM DTT, and 0.1 mM phenylmethylsulfonyl fluoride, and developed using 200 ml of a linear gradient up to 1 M NaCl. NC-dUTPase appeared at 0.35–0.5 M NaCl. Superdex 200 HR column gel filtration was carried out in 20 mM Hepes buffer (pH 7.0) containing 500 mM NH_4Cl, 2 mM DTT, 10 mM β-mercaptoethanol, and 25 mM $MgCl_2$. The purified preparations appeared as single bands on SDS-PAGE, gel densitometry suggested at least 95% purity. Enzyme stocks were concentrated on Millipore centrifugal filters (10 kDa cutoff) to a final concentration of 5–15 mg/ml, flash-frozen in liquid nitrogen, and stored at −70 °C. As shown by activity measurements and SDS-PAGE, this storage did not cause considerable degradation up to three months, but precipitation became prominent after cycles of freeze/thaw. Throughout the present study, molar enzyme concentrations refer to the monomeric species, unless stated otherwise. Before use, aliquots of the enzyme were dialyzed against respective buffers.

Protein concentration was measured by Bradford's assay (26) or spectrophotometrically using $A^{0.1\%}$ 1 cm, 280 nm = 0.74 or 0.76 for NC-dUTPase, or dUTPase, respectively, as calculated from amino acid composition. UV absorbance spectra were recorded on a JASCO-V550 spectrophotometer at 25 °C in 20 mM HEPES buffer (pH 7.0) also containing 500 mM NH_4Cl, 2 mM DTT, 10 mM β-mercaptoethanol, and 25 mM $MgCl_2$.

dUTPase Activity Assay by Thin Layer Chromatography—Reactions were with 1 μM dUTPase in 20 mM HEPES buffer (pH 7.5) containing 150 mM KCl, 5 mM $MgCl_2$, and 10 mM of either dUTP, dCTP, or dTTP. At time points, 0.5–1 μl of the reaction mixtures was spotted on Baker-flex silica gel IB2-F thin layer plates. Plates were developed in 6:3:1 iso-propanol/NH_3/H_2O, resulting in approximate retention values in percent of distance traveled from start point related to total distance traveled by the eluent of 40, 11, and 5% for dNMP, dNDP, and dNTP, respectively. Spots were visualized under UV light.

Continuous Spectrophotometric dUTPase Activity Assay—Proton release during the transformation of dUTP into dUMP and PP_i was followed at 559 nm at 25 °C (19), using a JASCO-V550 spectrophotometer. Reaction mixtures contained 240 nM enzyme in 1 mM Tes-HCl (pH 7.5) containing 40 μM dUTP, 0.1–5 mM $MgCl_2$, 150 mM KCl, and 40 μM Phenol Red indicator (assay buffer). Initial velocity was determined from the slope of the first 10 s of the progress curve. The enzyme kinetic parameters k_{cat} and K_M were also determined from the entire progress curve using the integrated Michaelis-Menten equation (27, 28). Metal ion requirement was tested in separate experiments, using components run through a 50-ml Chelex column (1 ml/min flow rate).

Dynamic Light Scattering—Measurements were carried out on a DynaPro-MS/X molecular sizing instrument (Protein Solutions, Inc., VA) with a 20-μl micro-sampling cell at 20 °C, according to the manufacturer's recommendations. The sample contained 1.1 mg/ml protein in 20 mM HEPES buffer (pH 7.0) containing 200 mM NH_4Cl, 1 mM $ZnCl_2$, 2 mM DTT, and 10 mM β-mercaptoethanol. An aliquot of 25 μl was freshly filtered (0.02 μm Whatman Anodisc (Whatman, UK)) into the measurement cell. One hundred readings were recorded, and the data were analyzed using the non-negatively constrained least squares method (29) incorporated into the DYNAMICS version 5.20.05. The analysis is based on the Stokes-Einstein equation ($D_T = k_bT/6\ P_i(SV)R_H$), under the assumption of Brownian motion. D_T (translational diffusion coefficient) was converted to the hydrodynamic radius (R_H) of the sample particles (k_b is Boltzmann's constant, T is the absolute temperature in degrees Kelvin, P_i is the value of the constant Pi, and (SV) is the solvent viscosity). Polydispersity was defined as (standard deviation of R_H)/R_H, giving an estimation of the homogeneity of particle sizes in the sample (30).

Analytical Gel Filtration—A Superdex 200 HR column, calibrated with transferrin, ovalbumin, myoglobin, and RNase (molecular masses: 81, 43, 17.6, and 13.7 kDa, respectively). 500 μl samples were applied at 0.1–1.0 mg/ml protein concentrations. Exclusion volume was determined by using blue dextran.

PAGE—SDS-PAGE was performed using 12–18% minigels. Protein bands were visualized by colloidal Coomassie Brilliant Blue (Bio-Rad) and quantitated on a GelDoc densitometer (Bio-Rad). Native PAGE on

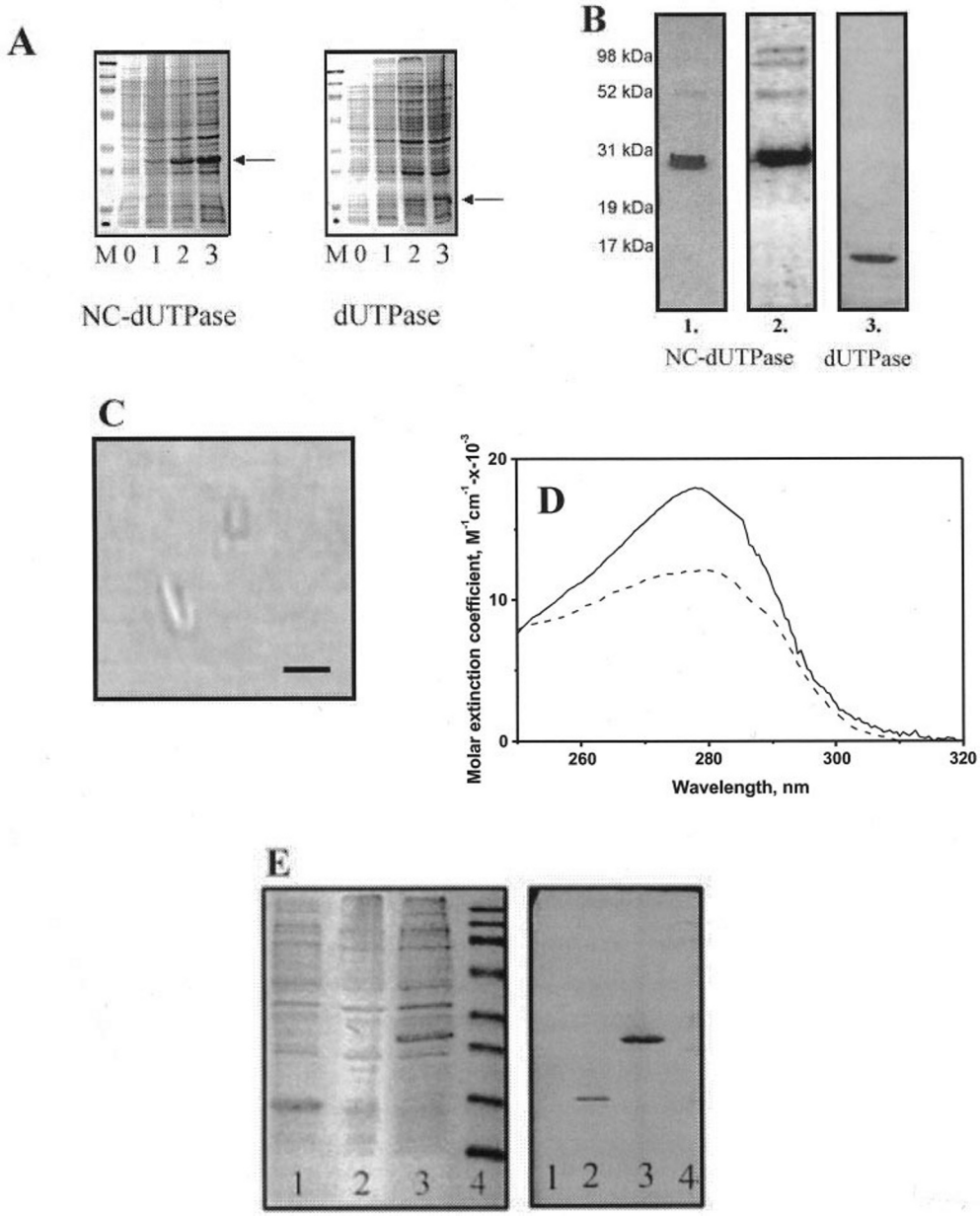

FIG. 1. Expression (*A*), purification (*B*), crystallization (*C*), and spectroscopy (*D*) of recombinant NC-dUTPase and dUTPase. *A*, bacterial cell extracts were loaded on SDS-PAGE before induction (*lanes 0*), as well as one, two, and three hours after induction (*lanes 1*, *2*, and *3*). *M* stands for molecular mass marker (205, 116, 66, 45, 29, 20, 14.2, and 6.5 kDa). *Arrows* indicate the positions of the NC-dUTPase and dUTPase proteins. Note the difference between expression patterns. *B*, recombinant proteins after purification. *Numbers* indicate positions of molecular mass standards. *Lane 1* and *3*, SDS-PAGE. *Lane 2*, Western blot developed with antiserum against M-PMV dUTPase. *C*, single crystals of M-PMV dUTPase. Mark length is 0.1 mm. *D*, UV absorption spectra of NC-dUTPase (*solid line*) and dUTPase (*dashed line*). The molar extinction coefficients at 280 nm, 18,250 and 12,160 $M^{-1}cm^{-1}$ for NC-dUTPase and dUTPase, respectively, calculated from the amino acid composition, were used to scale the spectra of protein solutions, recorded in absorbance units, to molar values. *E*, characterization of the polyclonal antiserum raised against M-PMV dUTPase. *E. coli* extracts from strains overproducing *E. coli* dUTPase (57) (*lane 1*), M-PMV dUTPase (*lane 2*), and M-PMV NC-dUTPase (*lane 3*) were probed with the rabbit polyclonal antibody raised against M-PMV dUTPase. Note that only bands corresponding to the M-PMV NC-dUTPase and dUTPase react with the antiserum. *Lane 4*, prestained molecular mass marker (205, 116, 66, 45, 29, 20, 14.2, and 6.5 kDa). The stain of the marker is retained on the blot.

Novex 10% polyacrylamide gel pre-casted with Tris borate-EDTA buffer (Invitrogen) was run in reverse direction in 0.2 M sodium-acetate buffer (pH 4.5).

Circular Dichroism (CD) Measurements—Far UV CD spectra were recorded on protein samples at 0.2 mg/ml concentration in 20 mM Tris buffer (pH 8.0) containing 200 mM NH_4Cl, and 5 mM DTT. 1–4 μl aliquots of concentrated and buffered $Zn(Ac)_2$ solution were added in the cuvette to reach the final concentrations. Three scans were averaged.

N-terminal Microsequencing—Protein samples blotted on polyvinylidene fluoride membrane were analyzed at the Analysis and Synthesis Laboratory of the Agricultural Biotechnological Research Center of Gödöllö, Hungary on ABI 471A of Applied Biosystems, Inc.

Antiserum Production and Western Blotting—Rabbits were immunized with recombinant M-PMV dUTPase. For the first injection, antigen in complete Freund's adjuvant was injected into the muscle of the upper thigh of the animals. The second injection was carried out 3 weeks later using incomplete Freund's adjuvant, followed by boosting at a 2-week interval, using antigen solution in physiological saline. Serum was used at a dilution of 1:50,000 in Western blots on nitrocellulose membranes. Antisera against M-PMV NC and capsid proteins were kindly provided by Dr. T. Ruml from the Institute of Chemical Technology, Prague, Czech Republic. Blots were stained first with Ponceau dye and then developed with the antiserum, followed by staining with secondary antibody (alkaline phosphatase or horseradish peroxidase labeled anti-rabbit IgG). For visualization, nitro-blue-tetrazolium/5-

bromo-4-chloro-3-indolyl phosphate or the enhanced chemiluminescence kit of Amersham Biosciences, respectively, was used.

Purification of M-PMV Virions—The rhesus monkey CMMT cell line, chronically infected with M-PMV, was grown in Dulbecco's essential medium with 10% fetal bovine serum. Medium containing released virions was collected from confluent plates and filtrated through a membrane filter (0.45 μm). Virions were pelleted through a 15% (m/vol) sucrose cushion for 1 h at 160,000 $\times$ *g*. The virus pellet was resuspended in 10 mM Tris buffer (pH 7.6) containing 500 mM NaCl and 1% (v/v) Triton X-100, and loaded onto sucrose velocity gradient containing 25–60% (m/vol) sucrose in the same buffer. The gradient was centrifuged at 160,000 $\times$ *g* for 1 h at 4 °C, and 1 ml fractions were collected from the top of the gradient. Fractions were analyzed by SDS-PAGE and Western blot.

Analysis of Virus Proteins in Infected COS-1 Cells—Confluent CMMT cells, chronically infected with M-PMV, were incubated in Cys, Met-free Dulbecco's modified Eagle's medium (Sigma) (30 min, 37 °C) followed by change into medium containing ^{35}S-labeled methionine and cysteine (60 μCi/ml) (ICN) for overnight labeling (31). Radiolabeled virus particles were filtered through 0.45 μm polysulfone membrane, and 10 μg/ml of polybrene was added. COS-1 cells were overlaid with the radiolabeled virion mixture and incubated for 2 h at 37 °C, washed several times, and complete Dulbecco's modified Eagle's medium was added. Cells were lysed after 4 h in 50 mM Tris-HCl (pH 7.5) buffer containing 1% Triton X-100, 1% sodium-deoxycholate, 0.15 M NaCl, mixture protease inhibitor mix, 7 μg/ml DNase, and 15 μg/ml RNase (lysis buffer A). Cell-associated viral proteins were immunoprecipitated from the lysate using the M-PMV dUTPase antiserum and protein A agarose in the presence of 0.1% SDS. Radiolabeled viral proteins from the immunoprecipitate were separated on SDS-PAGE and detected by autoradiography. In a separate experiment, COS-1 cells were infected with non-labeled released virions from confluent CMMT cells in the presence of polybrene (10 μg/ml). Cells were lysed after washing in lysis buffer at different time (1, 2, 4, and 6 h), and cell-associated proteins were separated on SDS-PAGE and detected by Western blot using SuperSignal West-femto sensitivity substrate (Pierce).

Cleavage of M-PMV NC-dUTPase Protein by M-PMV Protease in Vitro—The purified NC-dUTPase was dialyzed against 50 mM phosphate buffer (pH 6.2) containing 300 mM NaCl and 0.01% (v/v) β-mercaptoethanol and was concentrated to 0.3 mg/ml. Reaction mixture contained 33 μM NC-dUTPase in a total volume of 40 μl and 2 μM M-PMV protease, expressed and purified as described previously (32). Following an overnight incubation at 37 °C, reaction products were analyzed by SDS-PAGE and Western blots.

Crystallization—Conditions were screened at different temperatures (Crystal Screen, Hampton Research). Vapor diffusion experiments were made in hanging drops against 500 μl reservoir. dUMP was added to the enzyme solution (7.4 mg/ml protein in 20 mM Tris buffer (pH 7.05) containing 0.5 M NaCl and 1 mM DTT) in equimolar amounts (relative to the monomer). Enzyme solutions (2 μl) were mixed with an equal amount of the reservoir solution.

Preliminary X-ray Analysis—Synchrotron radiation was used to collect diffraction data at 100 K from a cryoprotected flash-frozen crystal. Measurements were carried out at beam ID29 European Synchrotron Radiation Facility (Grenoble, France) using ADSC Q210 CCD detector. Cell parameters and crystal system were determined by MOSFLM 6.01 program (33). Matthews coefficient and solvent content of the crystal were calculated with the CCP4 program suite (34).

RESULTS

Cloning, Expression, and Antibody Production—Fig. 1*A* shows the expression patterns of the constructs NC-dUTPase and dUTPase. The yields of the proteins were 120 mg/liter and 30 mg/liter, respectively. This lower yield for dUTPase was considerably improved upon silent mutagenesis of CGG^{Arg} and GGG^{Gly} (data not shown). DNA sequencing of the plasmids was in complete agreement with the desired sequences, and N-terminal microsequencing of the expressed proteins also gave the expected results (KRVEG for dUTPase, AAAFSGQTVKP for NC-dUTPase). Molecular mass estimated from SDS-PAGE is 16 kDa, and 27 kDa for dUTPase, and NC-dUTPase, respectively. These data indicate that the recombinant constructs faithfully represent the dUTPase and NC-dUTPase proteins of M-PMV retrovirus. Fig. 1*B* shows the SDS-PAGE of the purified proteins. The faint higher band in the NC-dUTPase lane is due to a cross-linked aggregate of NC-dUTPase as it was shown to react with the antibody developed against M-PMV dUTPase (Fig. 1*E*). No cross-reactivity of this polyclonal serum to dUTPases from other species, or to other proteins was detectable. As an ultimate test of protein purity, Fig. 1*C* demonstrates that single crystals of purified M-PMV dUTPase can be crystallized. Following several chromatographic steps, the proteins were also practically free from nucleic acid contaminations, as shown by the UV absorbance spectra (Fig. 1*D*) where the maximum wavelength of absorbance is around 280 nm (characteristic for aromatic amino acid side chains).

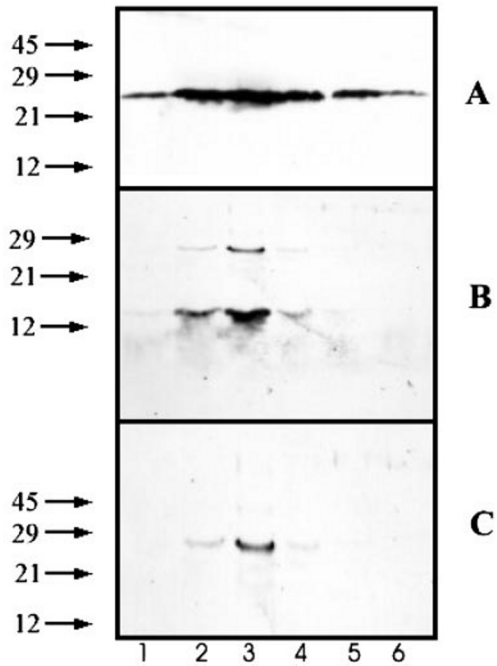

FIG. 2. **Western blots of proteins in M-PMV virions probed with antisera against capsid (*A*), NC (*B*), and dUTPase proteins (*C*).** Fractions from the sucrose gradient step of the M-PMV virion purification were examined for presence of M-PMV viral proteins. *Arrows*, marker positions.

M-PMV Virions and Infected Cells Contain NC-dUTPase, Resistant to Cleavage with Either M-PMV or Cellular Protease—To determine the status of dUTPase in M-PMV virions, immunoblot analysis of virion-associated proteins from sucrose gradient fractions was performed using antibodies against NC (Fig. 2*B*) and dUTPase (Fig. 2*C*). Western blot analysis of M-PMV viral proteins using antibodies agains M-PMV capsid revealed that gradient fractions 2–4 (corresponding to 31–39% (m/vol) sucrose, or 1.13–1.17 g/ml density) contained the peak of M-PMV-associated proteins (Fig. 2*A*). These fractions, when reacted with anti-NC antiserum, were shown to contain NC in two forms, characterized by 27 kDa (at relative amount of 12%) and 13 kDa (at relative amount of 88%) (Fig. 2*B*, *lanes 2–4*). The 27-kDa form co-localizes with the only band showing reactivity with the mono-specific antiserum developed against M-PMV dUTPase (Fig. 2*C*, *lanes 2–4*). These results indicate that mature M-PMV virions contain the fusion protein NC-dUTPase as the only detectable source of dUTPase, whereas NC protein is present both as fused to dUTPase (27 kDa form) and in free (13 kDa) form.

To investigate if M-PMV protease, which cleaves viral polyproteins during maturation, is able to cleave NC-dUTPase under optimal *in vitro* conditions, purified NC-dUTPase was incubated with recombinant M-PMV protease. Fig. 3, *A* and *B*, show that no cleavage of NC-dUTPase occurs even upon prolonged incubation with the protease. It can be concluded that

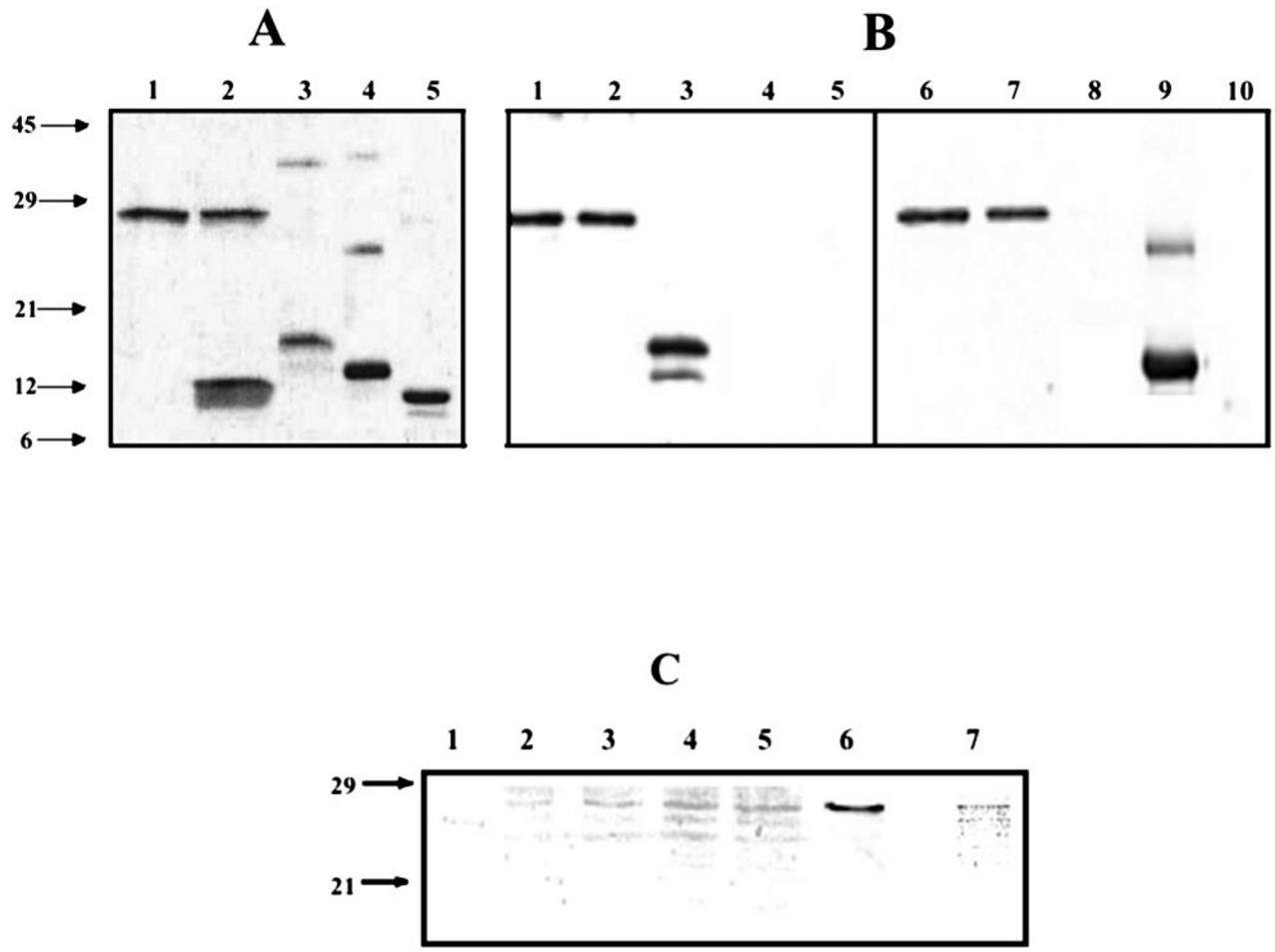

FIG. 3. **Lack of proteolytic processing of M-PMV NC-dUTPase *in vitro* and in infected COS-1 cells.** *A* (SDS-PAGE) and *B* (Western blot) show analysis of *in vitro* proteolytic processing of M-PMV NC-dUTPase by retroviral M-PMV protease. *Lanes 1* and *6*, NC-dUTPase before incubation with protease; *lanes 2* and *7*, NC-dUTPase after incubation with protease; *lanes 3* and *8*, dUTPase; *lanes 4* and *9*, NC; *lane 5* and *10*, protease. *Lanes 1–5* in *B* were probed with M-PMV dUTPase antiserum, *lanes 6–10* with M-PMV NC antiserum. *C,* Western blot analysis (*lanes 1–6*) and autoradiograph of metabolically labeled and immunoprecipitated protein (*lane 7*) with rabbit anti-dUTPase. *Lane 1*, mock-infected cells; *lane 2*-5, cell lysates 1, 2, 4, and 6 h after infection of COS-1 cells with M-PMV virions released from CMMT cells; *lane 6*, virions released from C-MMT cells; *lane 7*, protein immunoprecipitated from COS-1 cells 4h after infection with metabolically labeled [^{35}S]M-PMV.

the NC-dUTPase junction is practically fully resistant to proteolysis by the retroviral protease.

To determine whether NC-dUTPase might get cleaved by cellular proteases in infected cells, we have analyzed M-PMV cell-associated proteins. Radiolabeled M-PMV virions released from CMMT cells were used to infect COS-1 cells. Viral proteins were immunoprecipitated from COS-1 lysate with rabbit anti-dUTPase. The immunoprecipitate was analyzed by SDS-PAGE followed by autoradiography (Fig. 3*C*, *lane 7*) to reveal the presence of one significant protein band, migrating at ~27 kDa. This apparent molecular mass corresponds to the size of the intact NC-dUTPase fusion protein (see Fig. 3*C*, *lane 6*). Western blot analysis of COS-1 cell-associated proteins using anti-dUTPase antibody and chemiluminescent substrate also showed one protein band reactive to anti-dUTPase that migrates at 27 kDa (Fig. 3*C*, *lanes 2–5*). These results confirm that NC-dUTPase is not degraded within the cells and also show that the highest level of NC-dUTPase was detected within the cells 4 h after infection (Fig. 3*C*, *lanes 4* and *5*). Results indicate that i) M-PMV virions produced by the chronically infected CMMT cell line can infect COS-1 cells, and ii) no degradation of NC-dUTPase by cellular proteases is detectable in infected cells.

Enzyme Kinetic Studies—Michaelis-Menten parameters for dUTP cleavage do not differ for NC-dUTPase and dUTPase (Table I). Mg^{2+} is a co-factor for both constructs, whereas Zn^{2+}, a known strong chelator of the NC domain, does not have an appreciable effect. Zn^{2+} was applied at relatively low concentration to prevent precipitation, but this concentration assured binding of the ion to NC as shown by CD spectroscopy (see Fig. 5 and text below). k_{cat} is very low (0.6 s^{-1}), similar to the value obtained for MMTV NC-dUTPase (16, 17). Specificity studies with the close substrate analogues dCTP and dTTP showed that k_{cat} is further decreased by one order of magnitude (0.05 s^{-1} and 0.03 s^{-1}, respectively), making K_M. Determinations unreliable due to the very slow reaction. No change in specificity could be seen when comparing NC-dUTPase and dUTPase. To check if binding of an oligonucleotide to the NC domain might modulate dUTPase activity within the fusion NC-dUTPase protein, a hexanucleotide (ACTGCC) was synthesized. This hexanucleotide binds with high affinity to the closely similar NC protein of human immunodeficiency virus (35), and the amino acid residues involved in oligonucleotide binding were identified in the three-dimensional structure (36). Most of these residues are present in M-PMV NC protein as well. The hexanucleotide was added at the concentration required to provide possibly full complexation of NC protein (published dissociation constants of 100–500 nM, see Refs. 37 and 38). Other studies of DNA-NC protein interaction reported high preference of NC for binding to TG dinucleotide repeats (39, 40). Therefore the octanucleotide $(TG)_4$ was also synthesized and used in parallel experiments. Table I shows that both

TABLE I

Kinetic parameters of M-PMV dUTPase and NC-dUTPase, as measured in the enzyme-catalyzed cleavage of dUTP, in the presence 100 μM $MgCl_2$ and different additives

Data represent average and error of 5-8 parallel measurements. Hexanucleotide sequence, ACTGCC; octanucleotide sequence, TG.

Enzyme	Additives	k_{cat} (s^{-1})	k_{cat}/K_M (M^{-1} s^{-1})
dUTPase	none	0.65 ± 0.17	(3.2 ± 0.5) × 10^5
NC-dUTPase	none	0.68 ± 0.20	(3.6 ± 0.4) × 10^5
	50 μM $Zn(Ac)_2$	0.60 ± 0.12	(2.8 ± 0.5) × 10^5
	50 μM $Zn(Ac)_2$ + 10 μM hexanucleotide	1.2 ± 0.25	(10.5 ± 1.5) × 10^5
	50 μM $Zn(Ac)_2$ + 10 μM octanucleotide	0.85 ± 0.22	(12.3 ± 2.4) × 10^5

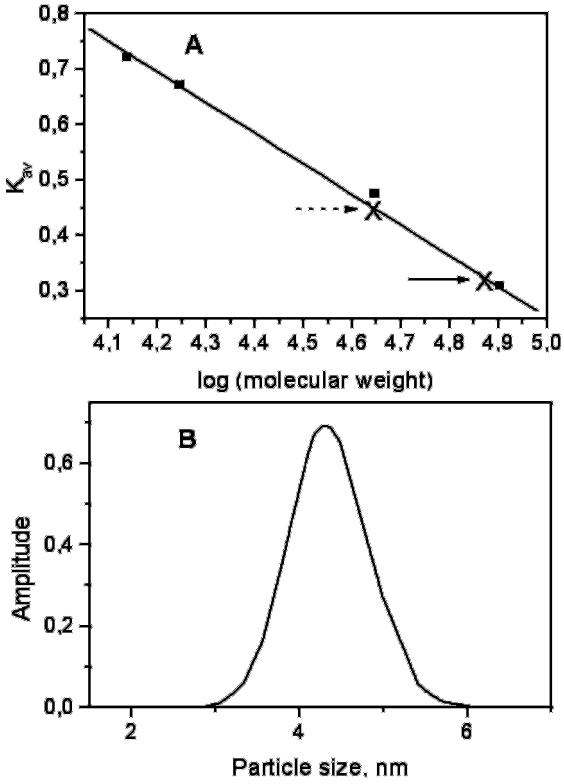

FIG. 4. **Oligomerization status of NC-dUTPase and dUTPase.** *A*, analytical gel filtration. K_{av} was calculated according to the equation $(V_e - V_0)/(V_T - V_0)$, where V_e is the elution volume, V_0 is the exclusion volume, and V_T is the total volume of the column. *Solid line* shows the linear function of K_{av} as obtained with the calibration proteins (*closed squares*). *Arrows* indicate the positions of NC-dUTPase (*solid*) and dUTPase (*dashed*), respectively. *B*, dynamic light scattering. Results shown were obtained with NC-dUTPase. The observed average particle size is 4.20 nm, the estimated molecular weight is 93 kDa, and the polydispersity is 18.5%.

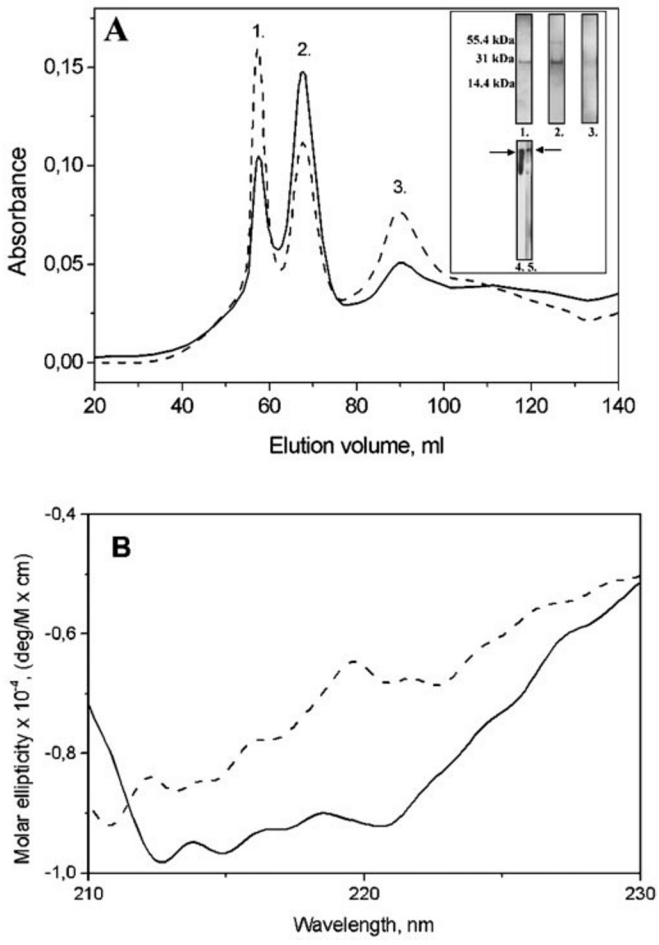

FIG. 5. **Binding of nucleocapsid-cognate ligands to NC-dUTPase.** *A*, gel filtration of ion exchange purified NC-dUTPase. Three peaks (*1*, *2*, and *3*) are identified in the chromatograms showing A_{260} (*dashed line*) and A_{280} (*solid line*). *Inset*, *lanes 1*, *2*, and *3* show SDS-PAGE analysis of the three peaks of the gel filtration curve. *Lanes 4* and *5* correspond to the same native gelelectrophoretogram of the sample from the gel filtration peak 1, stained with ethidium bromide to show DNA presence (*negative image*, *lane 4*), or with Coomassie Blue to show protein presence (*lane 5*). *B*, far UV circular dichroism spectra of M-PMV NC-dUTPase alone (*solid line*) and in the presence of 40 μM $Zn(Ac)_2$ (*dotted line*).

oligonucleotides have a slight, but appreciable, positive modulating effect on NC-dUTPase, in the simultaneous presence of Mg^{2+} and Zn^{2+}. A 10-fold increase in oligonucleotide concentration had no further effect. The presence of the oligonucleotide had no effect on the activity of NC-lacking dUTPase in either of the combinations tested (data not shown), in agreement with the expectation that oligonucleotide binding-induced effects are probably mediated by the NC domain. These results indicate that i) the low activity of M-PMV dUTPases is an inherent property not due to the nucleocapsid domain, and ii) NC-dUTPase activity may be modulated by oligonucleotide binding to the NC segment. To account for the low activity, correct folding of the protein constructs was checked by circular dichroism spectroscopy.

Estimation of Secondary Structure by CD Spectroscopy—CD spectra recorded in the peptide bond absorption wavelength range reflect secondary structural elements with reasonable accuracy (41, 42). Spectra of M-PMV NC-dUTPase and dUTPase were processed by the k2d program (42), previously shown to describe secondary structural content for *E. coli* dUTPase in agreement with the crystal structure (27). Results indicate that both M-PMV dUTPase and NC-dUTPase contain a high amount of β-structure (41 and 38%, respectively), and a low amount of α-helices (6 and 8%, respectively). These values are very close to those determined for *E. coli* dUTPase (5% α-helix, 42% β-structure (27)), indicating that an intact dUTPase-like fold may be present in both recombinant M-PMV proteins. The α-helical content is very low for both M-PMV proteins, which seems to indicate that the helices of the NC domain do not

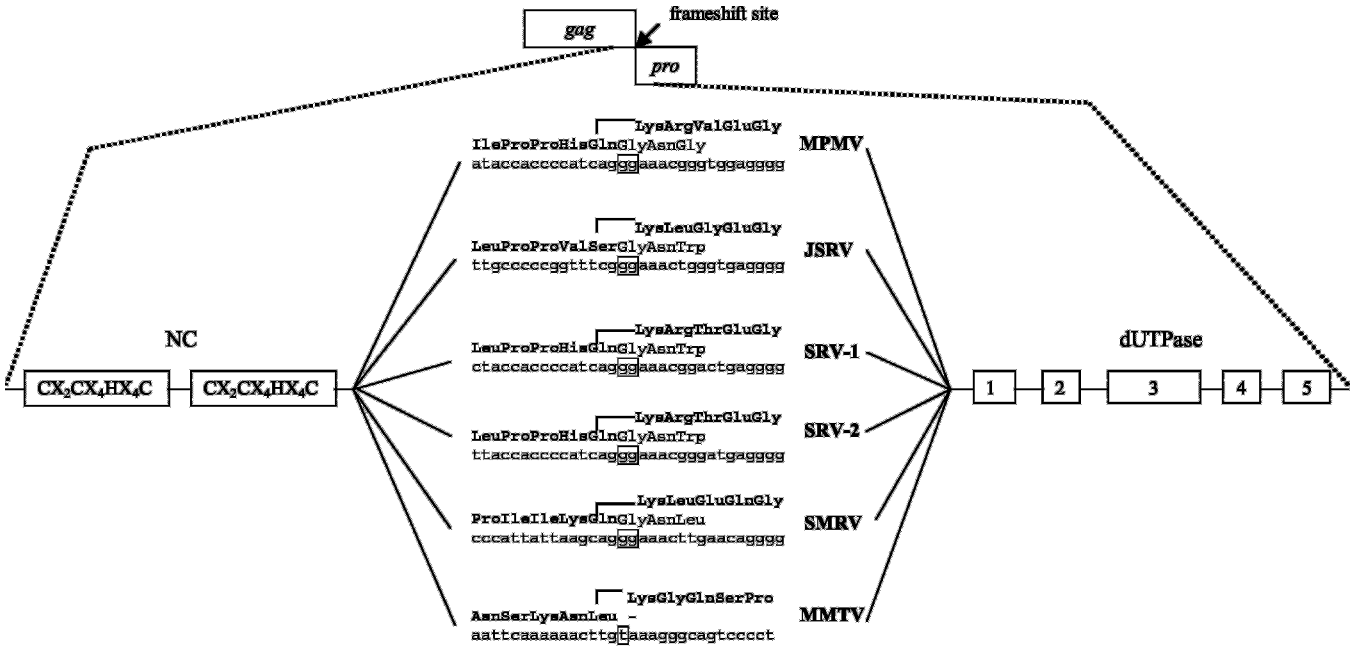

FIG. 6. **Gag-pro frameshift site conservation in betaretroviral genomes.** Ribosomal frameshift (*boxed letters* in the nucleotide sequences) occurring at ~12% frequency at the *gag-pro* junction leads to translation of the fusion protein NC-dUTPase. Betaretroviral genomes for which sequence data are available were investigated for the location of the frameshift site, which was experimentally mapped in the Mason-Pfizer monkey virus (*MPMV*) and MMTV genomes (47). In five out of six cases, the frameshift location drives the expression of the fusion protein NC-dUTPase in such a way that the last fifteen residues of NC as well as the full-length of protein p4 do not get translated. In the single case of MMTV, the frameshift occurs right at the stop codon (taa) after the NC gene. GenBank™ data were used for sequences of *M-PMV* (M12349), *JSRV* (Jaagsiekte sheep retrovirus) (M80216), *SRV-1* (simian retrovirus 1) (M11841), *SRV-2* (simian retrovirus 2) (M16605), *SMRV* (squirrel monkey retrovirus) (M23385), and *MMTV* (M15122). *Boxed elements* before and after the frameshift site show consensus sequence of the Zn-knuckle motifs in the NC region and the five conserved motifs in the dUTPase region.

significantly contribute to the CD signal. This is not surprising, as the expected helical content with completely folded α-helices of the NC domain, estimated from the three-dimensional structure as determined by NMR (43) would not exceed 5% in the whole length NC-dUTPase. In conclusion, CD spectra are in agreement with a correctly folded dUTPase domain that is not heavily perturbed by the NC domain.

Oligomerization Status—dUTPase active site architecture ultimately depends on quaternary organization (see the Introduction). Incorrect oligomerization may therefore decrease catalytic activity. Gel filtration data indicate native molecular masses of 78 and 46 kDa for NC-dUTPase and dUTPase, respectively (Fig. 4*A*). Dynamic light scattering measurements provided an independent estimate of 93 kDa for NC-dUTPase (Fig. 4*B*), somewhat higher than the result from the gel filtration experiment. If the shape of the oligomer is appreciably non-spherical, its mass may be overestimated by light scattering. Together with the subunit molecular mass data (27 kDa for NC-dUTPase and 16 kDa for dUTPase, Fig. 1*B*), the homotrimeric quaternary structure can be ascertained for both M-PMV dUTPase and NC-dUTPase with high probability. This result indicates that the homotrimer is correctly assembled.

Binding of Cognate Ligands of the Nucleocapsid Domain to NC-dUTPase (Fig. 5)—Nucleocapsid is a well known nucleic acid-binding protein, containing two tandem CCHC Zn-knuckle motifs (37, 38). During purification of recombinant NC-dUTPase, a considerable amount of nucleic acids was co-purified with the protein during cation exchange chromatography. During gel filtration, a considerable amount of NC-dUTPase protein appeared in complex with nucleic acids (Fig. 5*A*). On the contrary, NC-lacking dUTPase was essentially nucleic acid-free following cation exchange chromatography. Results indicate that nucleic acid binding ability is present in NC-dUTPase.

Binding of Zn^{2+} to the Zn-knuckle Motifs within NC Was Investigated by CD Spectroscopy (Fig. 5B)—Upon Zn^{2+} addition, a characteristic increase in the CD signal at 230–210 nm wavelength range, shown to be induced by Zn^{2+} binding to NC protein in several independent laboratories (44–47), is readily recognizable in the spectra of NC-dUTPase. Results indicate that both nucleic acid and Zn^{2+} binding, characteristic for NC, are retained in the M-PMV NC-dUTPase fusion protein.

Crystallization and Preliminary Crystallography—A high-resolution three-dimensional structure would provide a structural explanation for the low specific activity. Crystallization of M-PMV dUTPase was therefore attempted. Crystals grew best in hanging drops with salt (sodium-formate, sodium-acetate, or Li_2SO_4) as precipitant. Crystals used for x-ray analysis with dimensions of 0.1 × 0.05 × 0.05 mm were obtained at 4 °C in the presence of 0.1 M sodium-acetate buffer (pH 4.6) with 2.0 M sodium-formate (see Fig. 1*C*). Crystals 5-fold larger in each dimension have also been obtained recently. Despite widespread crystallization attempts with NC-dUTPase, no crystals could yet be obtained in this case.

Preliminary X-ray diffraction analysis at synchrotron radiation (beyond 3.7 Å) proves that the space group is either primitive trigonal or primitive hexagonal, with cell dimensions a = b = 60.83 Å, c = 64.03 Å, $\alpha = \beta = 90°$, $\gamma = 120°$. Collection of complete data sets is in progress. This requires multiple crystals due to short lifetime in the x-ray beam. Assuming 6 monomers per unit cell, calculation of Matthews coefficient gives 2.47 $Å^3\ Da^{-1}$ together with a solvent content of ~50.2%, which are normal values for globular proteins (48). The type of the space group argues for the presence of 3-fold symmetry in the crystal. This suggests that the trimeric arrangement, typical to well described representatives of the dUTPase family, and shown to exist in solution for M-PMV dUTPase as well (Fig. 4*A*), is retained in the crystal phase.

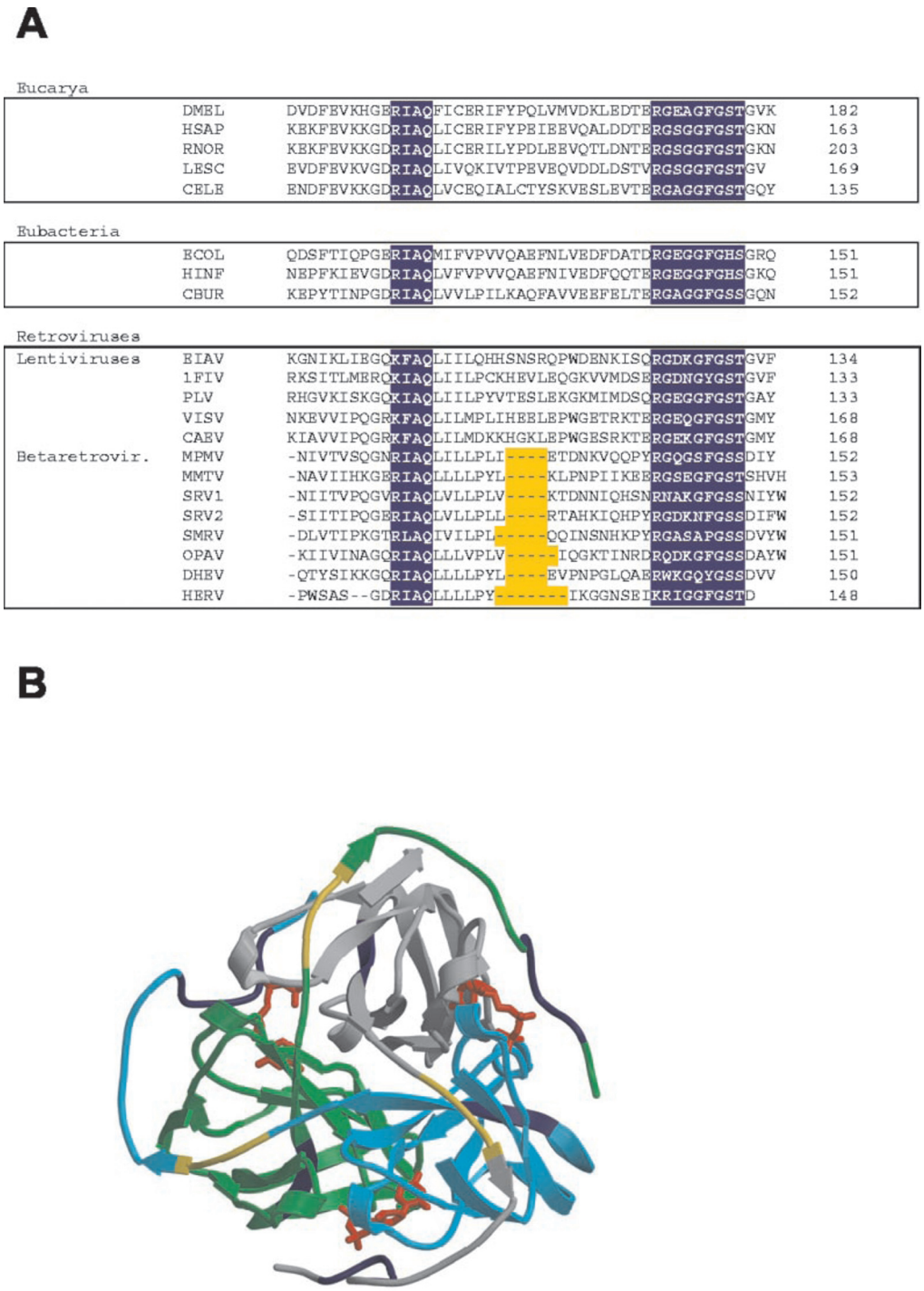

FIG. 7. **Shortened spacer in betaretroviral dUTPases.** *A*, alignment of dUTPase sequences in the region of conserved motifs 4 and 5. Eukaryotic, bacterial, lentiviral, and betaretroviral sequences are shown. *Dark blue background* indicates conserved motifs 4 and 5; *yellow background* is for the gaps in the betaretroviral sequences in the spacer separating motif 4 and 5. *DMEL*, *Drosophila melanogaster* (55); *HSAP*, *Homo sapiens* SwissProt P33316; *RNOR*, *Rattus norvegicus* SwissProt U64030; *LESC*, *Lycopersicon esculentum* SwissProt P32518; *CELE*, *Caenorhabditis elegans* SwissProt U96695; *ECOL*, *E. coli* SwissProt P06968; *HINF*, *Haemophilus influenzea* SwissProt U32776; *CBUR*, *Coxiella burnettii* SwissProt S44300; *EIAV*, Equine infectious anemia virus (GenBank™ accession M16575); *1FIV*, feline immunodeficiency virus (GenBank™ accession M25381); *PLV*, puma lentivirus (GenBank™ accession PLU03982); *VISV*, visna/maedi virus (GenBank™ accession M60609); *CAEV*, caprine encephalitis virus (GenBank™ accession M33677); *MPMV*, Mason-Pfizer monkey virus (GenBank™ accession M12349); *MMTV*, mouse mammary tumor virus (GenBank™ accession M15122); *SRV1*, simian retrovirus 1 (GenBank™ accession M11841); *SRV2*, simian retrovirus 2 (GenBank™ accession M16605); *SMRV*, squirrel monkey retrovirus (GenBank™ accession M23385); *OPAV*, ovine pulmonary adenocarcinoma virus (GenBank™ accession M80216); *DHEV*, dwarf hamster endogenous retrovirus (GenBank 164632); *HERV*, human endogenous retrovirus (53). *B,* structural model of feline immunodeficiency virus dUTPase in complex with dUDP (Protein Data Bank 1F7R) (56). Ribbon diagrams of the three subunits are color-coded with *green*, *cyan*, and *gray*. The nucleotide ligand is in rod model in *red*. Conserved sequence motifs 4 and 5 are in *dark blue*, and the segment lacking in betaretroviruses is colored *yellow*. The carboxyl terminus of each chain is located as closing over the dUDP molecule bound at the neighboring subunit.

DISCUSSION

Covalent Linkage of NC and dUTPase Is Provided by Correct Positioning of the Frameshift Signal—Retroviral polyproteins are cleaved during maturation by viral-encoded protease into separate polypeptides that frequently form non-covalent homo- or heterooligomers. In the present work, however, clear evi-

dence is presented for the existence of the transframe protein NC-dUTPase, which is not cleaved either during maturation by M-PMV protease or by cellular proteases within infected cells, or under optimal *in vitro* conditions by recombinant M-PMV protease (Figs. 2 and 3). In fact, the amino acid sequence in this connecting region (PPHQ*KRVE, where * indicates the peptide bond separating NC and dUTPase domains (15)) does not conform to the specificity requirements of M-PMV protease (49, 50). The first frameshift signal (G.GGA.AA at nucleotides 2311–2316) is located within the NC-coding region of the M-PMV genome. Ribosomal frameshifting results in the synthesis of the NC-dUTPase fusion protein within the Gag-Pro polyprotein, wherein the NC domain lacks fifteen C-terminal amino acid residues but still retains both Zn-knuckle motifs. The full size NC as well as the p4 protein are cleaved out from the Gag polyprotein during maturation and therefore can fully function in the replication of the virus. A comparison of available betaretroviral genomic sequences (Fig. 6) reveals that the frameshift site conservation is rather universal in this group of viruses. All genomes containing a coding sequence for the p4 protein after the NC sequence have a strictly conserved frameshift site (consensus sequence GGGAAAC) within the NC coding sequence. This observation argues that the resistance of the fused NC-dUTPase protein against retroviral proteolysis is a general feature among betaretroviruses that may have been engineered through evolution by positioning a frameshift site within the NC coding region to avoid an authentic protease-processing site between NC and dUTPase sequences.

Functionality of the Transframe Protein—Figs. 2 and 3 show that in mature M-PMV virions as well as in infected COS-1 cells, dUTPase is exclusively found to be fused to NC, whereas ~12% of the total NC content of the virion is present as NC-dUTPase. This ratio is in good agreement with the frameshift frequency at the *gag-pro* junction in betaretroviruses MMTV and human endogenous retrovirus (14, 51, 52). The careful guarantee for the covalent linkage of NC and dUTPase, as discussed above, may suggest a role for this fusion in modulating both nucleocapsid and dUTPase functions. Two independent approaches convincingly show that the NC-dUTPase protein is a homotrimer with specific dUTPase activity (Fig. 4), wherein the nucleic acid and Zn^{2+}-binding NC is retained (Fig. 5). By fixing three nucleocapsid polypeptides on a common trimeric core provided by the dUTPase fold, the valency of the nucleic acid organizing unit is increased from one (single NC) to three (trimeric NC-dUTPase). Such a multivalent nucleic acid chaperone may compare positively with monovalent counterparts.

Inherent Low Catalytic Activity of Betaretroviral dUTPases—MMTV and M-PMV NC-dUTPases show similarly low k_{cat}/K_M values of 3–4 $\times$ 10^5 M^{-1} s^{-1} that is retained in the NC-lacking M-PMV dUTPase; therefore, it is not caused by the nucleocapsid domain but is an inherent property. Kinetic constants of M-PMV-MMTV and other dUTPases, these latter with k_{cat}/K_m values in the range of 2–5 $\times$ 10^7, reveals that k_{cat}/K_m decrease is mainly due to k_{cat} difference. k_{cat} of dUTPase from human endogenous retrovirus, a close relative of MMTV and M-PMV, is also in the same low range (0.7 s^{-1} (53)). k_{cat} values of other retroviral (54), bacterial (27, 28), and eukaryotic (*Drosophila melanogaster*)[2] enzymes are all much higher (8–15 s^{-1}). Although most, if not all, conserved dUTPase active site residues are present in M-PMV dUTPase as well (55), a detailed mutagenetic analysis is expected to reveal important clues regarding this difference. Sequence alignments point out a common feature in betaretroviral dUTPases: the spacer between motifs 4 and 5 is significantly decreased by 4–7 residues from the 21-residue length in all other dUTPases (Fig. 7*A*). This spacer crosses over to the substrate bound at the neighboring subunit to form the closed, catalytically competent enzyme conformer. The feline immunodeficiency virus dUTPase structure (56) reveals that spacer shortening may seriously compromise formation of the closed conformer (Fig. 7*B*). It is suggested that the diminished catalytic activity might be due to a steric constraint caused by the short spacer between the last two motifs. The success in crystallization and crystallography of M-PMV dUTPase (see "Results") will hopefully soon provide the required structural data. The experimental observation of the low catalytic activity inherent to the dUTPase domain relates the present work relevant for mechanistic investigations of dUTPases.

Whatever is the cause for the low activity, it should be compensated for under physiological circumstances. dUTPase levels in betaretroviruses and lentiviruses, the latter encoding high-activity enzyme (54), are not expected to differ considerably, because in both cases one frameshift with comparable frequency is required for dUTPase translation. We propose that compensation might be provided by adequate localization due to the NC domain. The present results indicated that the nucleic acid-binding ability is retained in the fusion NC-dUTPase, and that this may lead to positive modulation of enzyme activity. NC protein is known to associate to both the viral RNA and the *de novo* synthesized DNA strands during reverse transcription that requires fine-tuning of nucleotide pools. dUTPase anchored by NC to the reverse transcription machinery can fulfill its task of regulating local dUTP/dTTP ratios. By means of co-localization with the nucleic acids partaking in this process, dUTPase activity is used economically, and a low activity may still be enough to regulate local nucleotide pools.

Conclusion—Mature M-PMV virions are shown to contain NC and dUTPase proteins in stable covalent linkage giving rise to a homotrimer with an experimentally proven bifunctional character *in vitro*. Results indicate that nucleic acid binding and dUTP cleaving activities within the same protein may modulate both NC and dUTPase function.

Acknowledgments—We gratefully thank Prof. Eric Hunter for the gift of the viral vector pSARM4 and the CMMT cell line, Prof. Matthias Wilmanns, the EMBL Hamburg Outstation, and the European Community Program (Marie Curie Training Sites, HPMT-CT-20000-00174) for training (to O. B.), Dr. Veronika Harmat for early help in x-ray diffraction studies, Dr. Rebecca Persson for the gift of plasmid pECDUT, and Imre Zagyva for excellent technical assistance. Beam lines and operators at DW32 LURE (Orsay, France) and ID29 ESRF (Grenoble, France) are acknowledged for data collection opportunities.

REFERENCES

1. Pearl, L. H., and Savva, R. (1996) *Nat. Struct. Biol.* **3,** 485–487
2. Goulian, M., Bleile, B. M., Dickey, L. M., Grafstrom, R. H., Ingraham, H. A., Neynaber, S. A., Peterson, M. S., and Tseng, B. Y. (1986) *Adv. Exp. Med. Biol.* **195,** 89–95
3. el-Hajj, H. H., Zhang, H., and Weiss, B. (1988) *J. Bacteriol.* **170,** 1069–1075
4. Gadsden, M. H., McIntosh, E. M., Game, J. C., Wilson, P. J., and Haynes, R. H. (1993) *EMBO J.* **12,** 4425–4431
5. Lerner, D. L., Wagaman, P. C., Phillips, T. R., Prospero-Garcia, O., Henriksen, S. J., Fox, H. S., Bloom, F. E., and Elder, J. H. (1995) *Proc. Natl. Acad. Sci. U. S. A.* **92,** 7480–7484
6. Threadgill, D. S., Steagall, W. K., Flaherty, M. T., Fuller, F. J., Perry, S. T., Rushlow, K. E., Le Grice, S. F., and Payne, S. L. (1993) *J. Virol.* **67,** 2592–2600
7. Turelli, P., Guiguen, F., Mornex, J. F., Vigne, R., and Querat, G. (1997) *J. Virol.* **71,** 4522–4530
8. Pyles, R. B., Sawtell, N. M., and Thompson, R. L. (1992) *J. Virol.* **66,** 6706–6713
9. Steagall, W. K., Robek, M. D., Perry, S. T., Fuller, F. J., and Payne, S. L. (1995) *Virology* **210,** 302–313
10. Baldo, A. M., and McClure, M. A. (1999) *J. Virol.* **73,** 7710–7721
11. McClure, M. A., Johnson, M. S., and Doolittle, R. F. (1987) *Proc. Natl. Acad. Sci. U. S. A.* **84,** 2693–2697
12. McGeoch, D. J. (1990) *Nucleic Acids Res.* **18,** 4105–4110
13. Elder, J. H., Lerner, D. L., Hasselkus-Light, C. S., Fontenot, D. J., Hunter, E.,

[2] J. Kovári, O. Barabás, E. Takács, A. Békési, Z. Dubrovay, V. Pongrácz, I. Zagyva, T. Imre, P. Szabó, and B. G. Vértessy, manuscript in preparation.

Luciw, P. A., Montelaro, R. C., and Phillips, T. R. (1992) *J. Virol.* **66,** 1791–1794
14. Moore, R., Dixon, M., Smith, R., Peters, G., and Dickson, C. (1987) *J. Virol.* **61,** 480–490
15. Sonigo, P., Barker, C., Hunter, E., and Wain-Hobson, S. (1986) *Cell* **45,** 375–385
16. Koppe, B., Menendez-Arias, L., and Oroszlan, S. (1994) *J. Virol.* **68,** 2313–2319
17. Bergman, A. C., Bjornberg, O., Nord, J., Nyman, P. O., and Rosengren, A. M. (1994) *Virology* **204,** 420–424
18. Vertessy, B. G., Zalud, P., Nyman, P. O., and Zeppezauer, M. (1994) *Biochim. Biophys. Acta.* **1205,** 146–150
19. Vertessy, B. G., Persson, R., Rosengren, A. M., Zeppezauer, M., and Nyman, P. O. (1996) *Biochem. Biophys. Res. Commun.* **219,** 294–300
20. Prasad, G. S., Stura, E. A., McRee, D. E., Laco, G. S., Hasselkus-Light, C., Elder, J. H., and Stout, C. D. (1996) *Protein Sci.* **5,** 2429–2437
21. Mol, C. D., Harris, J. M., McIntosh, E. M., and Tainer, J. A. (1996) *Structure* **4,** 1077–1092
22. Larsson, G., Svensson, L. A., and Nyman, P. O. (1996) *Nat. Struct. Biol.* **3,** 532–538
23. Dauter, Z., Persson, R., Rosengren, A. M., Nyman, P. O., Wilson, K. S., and Cedergren-Zeppezauer, E. S. (1999) *J. Mol. Biol.* **285,** 655–673
24. Sambrook, J., and Russell, D. W. (2001) *Molecular Cloning: A Laboratory Manual*, Cold Spring Harbor Laboratory Press, New York
25. Studier, F. W., Rosenberg, A. H., Dunn, J. J., and Dubendorff, J. W. (1990) *Methods Enzymol.* **185,** 60–89
26. Bradford, M. M. (1976) *Anal. Biochem.* **72,** 248–254
27. Vertessy, B. G. (1997) *Proteins* **28,** 568–579
28. Larsson, G., Nyman, P. O., and Kvassman, J. O. (1996) *J. Biol. Chem.* **271,** 24010–24016
29. Morrison, I. D., Grabowski, E. F., and Herb, C. A. (1985) *Langmuir* **1,** 496–501
30. Ferre-D'Amare, A. R., and Burley, S. K. (1994) *Structure* **2,** 357–359
31. Rumlova, M., Ruml, T., Pohl, J., and Pichova, I. I. (2003) *Virology* **310,** 310–318
32. Zabransky, A., Andreansky, M., Hruskova-Heidingsfeldova, O., Havlicek, V., Hunter, E., Ruml, T., and Pichova, I. (1998) *Virology* **245,** 250–256
33. Leslie, A. G. W. (1992) Joint CCP4+ ESF-EAMCB, *Newsletter on Protein Crystallography*, **26**
34. Collaborative Computational Project Number 4 (1994) *The CCP4 Suite: Programs for Protein Crystallography, Acta Cryst.* **D50,** 760–763
35. Vuilleumier, C., Bombarda, E., Morellet, N., Gerard, D., Roques, B. P., and Mely, Y. (1999) *Biochemistry* **38,** 16816–16825
36. Morellet, N., Demene, H., Teilleux, V., Huynh-Dinh, T., de Rocquigny, H., Fournie-Zaluski, M. C., and Roques, B. P. (1998) *J. Mol. Biol.* **283,** 419–434
37. Dib-Hajj, F., Khan, R., and Giedroc, D. P. (1993) *Protein Sci.* **2,** 231–243
38. De Guzman, R. N., Wu, Z. R., Stalling, C. C., Pappalardo, L., Borer, P. N., and Summers, M. F. (1998) *Science* **279,** 384–388
39. Fisher, R. J., Rein, A., Fivash, M., Urbaneja, M. A., Casas-Finet, J. R., Medaglia, M., and Henderson, L. E. (1998) *J. Virol.* **72,** 1902–1909
40. Urbaneja, M. A., McGrath, C. F., Kane, B. P., Henderson, L. E., and Casas-Finet, J. R. (2000) *J. Biol. Chem.* **275,** 10394–10404
41. Greenfield, N. J. (1996) *Anal. Biochem.* **235,** 1–10
42. Andrade, M. A., Chacon, P., Merelo, J. J., and Moran, F. (1993) *Protein Eng.* **6,** 383–390
43. Gao, Y., Kaluarachchi, K., and Giedroc, D. P. (1998) *Protein Sci.* **7,** 2265–2280
44. Fitzgerald, D. W., and Coleman, J. E. (1991) *Biochemistry* **30,** 5195–5201
45. Surovoy, A., Dannull, J., Moelling, K., and Jung, G. (1993) *J. Mol. Biol.* **229,** 94–104
46. Omichinski, J. G., Clore, G. M., Sakaguchi, K., Appella, E., and Gronenborn, A. M. (1991) *FEBS Lett.* **292,** 25–30
47. Green, L. M., and Berg, J. M. (1990) *Proc. Natl. Acad. Sci. U. S. A.* **87,** 6403–6407
48. Matthews, B. W. (1968) *J. Mol. Biol.* **33,** 491–497
49. Hruskova-Heidingsfeldova, O., Andreansky, M., Fabry, M., Blaha, I., Strop, P., and Hunter, E. (1995) *J. Biol. Chem.* **270,** 15053–15058
50. Pichova, I., Zabransky, A., Kost'alova, I., Hruskova-Heidingsfeldova, O., Andreansky, M., Hunter, E., and Ruml, T. (1998) *Adv. Exp. Med. Biol.* **436,** 105–108
51. Jacks, T., Townsley, K., Varmus, H. E., and Majors, J. (1987) *Proc. Natl. Acad. Sci. U. S. A.* **84,** 4298–4302
52. Wang, Y., Wills, N. M., Du, Z., Rangan, A., Atkins, J. F., Gesteland, R. F., and Hoffman, D. W. (2002) *RNA* **8,** 981–996
53. Harris, J. M., McIntosh, E. M., and Muscat, G. E. (1999) *J. Mol. Biol.* **288,** 275–287
54. Bergman, A. C., Bjornberg, O., Nord, J., Rosengren, A. M., and Nyman, P. O. (1995) *Protein Expr. Purif.* **6,** 379–387
55. Fiser, A., and Vertessy, B. G. (2000) *Biochem. Biophys. Res. Commun.* **279,** 534–542
56. Prasad, G. S., Stura, E. A., Elder, J. H., and Stout, C. D. (2000) *Acta. Crystallogr. D. Biol. Crystallogr.* **56,** 1100–1109
57. Persson, R., Nord, J., Roth, R., and Nyman, P. O. (2002) *Prep. Biochem. Biotechnol.* **32,** 157–172